

Sum-Rate Maximization for IRS-Assisted UAV OFDMA Communication Systems

Zhiqiang Wei*, Yuanxin Cai*, Zhuo Sun†, Derrick Wing Kwan Ng*, and Jinhong Yuan*

*School of Electrical Engineering and Telecommunications, University of New South Wales

{zhiqiang.wei, yuanxin.cai, w.k.ng, j.yuan}@unsw.edu.au

†Research School of Electrical, Energy and Materials Engineering, Australian National University

zhuo.sun@anu.edu.au

Abstract—In this paper, we propose the use of intelligent reflecting surface (IRS) in unmanned aerial vehicle (UAV)-based orthogonal frequency division multiple access (OFDMA) communication systems. The proposed scheme exploits both the rich beamforming gain brought by the IRS and the high mobility of UAV for improving the system sum-rate. The joint design of UAV’s trajectory, IRS scheduling, and communication resource allocation for the proposed system is formulated as a non-convex optimization problem to maximize the system sum-rate. The existence of an IRS introduces both frequency-selectivity and spatial-selectivity in the fading of the composite channel from the UAV to ground users. To facilitate the design, we first derive the expression of the composite channel gain and propose a parametric approximation approach to establish a lower bound for the formulated problem. An alternating optimization algorithm is devised to handle the lower bound optimization problem. Simulation results unveil the promising sum-rate gain achieved by the deployment of an IRS in UAV-based communication systems.

I. INTRODUCTION

The recent advancement of unmanned aerial vehicles (UAV) manufacturing technologies has motivated extensive studies on the amalgamation between UAV and wireless communication systems [1]. Thanks to the high flexibility and the low-cost deployment of UAVs, efficient traffic offloading for terrestrial cellular networks can be performed which relieves system performance bottlenecks caused by overloaded traffic or blocked links. However, the performance of UAV-based communication systems is still restrained by the limited service duration and the users with weak communication links [2]–[4]. Recently, intelligent reflecting surface (IRS) has attracted extensive attention in the wireless communication research community, due to its capability of reshaping wireless propagation via establishing a programmable radio environment [5]. In particular, an IRS is a meta-surface constituted by a large number of passive reflection units (PRUs) and their impedance characteristics can be altered by an external IRS controller to adjust the amplitude and the phase of the reflected signals [6]. However, most of the existing works focused on IRS applications in terrestrial communications and their results cannot directly apply to emerging aerial communications.

The integration between the terrestrial IRS and UAV paves the way for the development of beyond fifth-generation (B5G) networks to offer ubiquitous communication services [7]. It is well-known that mounting multiple antennas at wireless

D. W. K. Ng is supported by funding from the UNSW Digital Grid Futures Institute, UNSW, Sydney, under a cross-disciplinary fund scheme and by the Australian Research Council’s Discovery Project (DP190101363).

transceivers can improve the performance of communication systems significantly. However, it is not cost-effective to allow a UAV to equip bulky multiple antennas, not to mention a power-hungry massive antenna array. In contrast, an IRS offers a high passive beamforming gain via adjusting its reflection coefficients intelligently, without the need to deploy multiple antennas on UAV. Therefore, the IRS can help “recycling” part of the dissipated signals by reflecting them back to the desired users. Secondly, deploying an IRS in UAV-enabled communication systems can improve the flexibility in designing UAV’s trajectory. For example, if a user is far away from the UAV but close to an IRS, the UAV does not have to deliberately alter its route and fly close to this far user for establishing strong communication links, which is usually time- and energy-consuming. Instead, an IRS can perform beamforming on the reflected signals jointly with the UAV to improve the received signal strength at the far ground user such that it can enjoy an acceptable data rate.

At the time of writing, there are only few initial works on IRS-assisted UAV communication systems to the best of the authors’ knowledge. For example, an IRS was deployed on a UAV in [8] to improve the communication reliability of terrestrial millimeter-wave systems. In particular, a reinforcement-based learning method was applied to optimize the position of the UAV and the reflection coefficients of the IRS to maximize the system sum-rate. In [9], the IRS was mounted on a building surface and served as a passive relay to assist UAV communication systems. The reflection coefficients of the IRS and the trajectory of the UAV were designed jointly to maximize the system sum-rate. A further extension to the case of multiple IRSs can be found in [10]. However, all these works [8]–[10] considered a narrow-band channel model and their results are not valid for wideband systems. Applying the existing results of [8]–[10] to multi-user wideband systems may result in unsatisfactory performance.

In this paper, we propose the application of an IRS to UAV-based orthogonal frequency division multiple access (OFDMA) communication systems and study the joint trajectory and resource allocation design to maximize the system sum-rate. Due to the reflected propagation path introduced by the IRS, the composite channel gains from the UAV to ground users becomes both frequency- and spatial-selective which complicates the trajectory design of the UAV. Via exploiting the cosine fading pattern in the composite channel power gains, we propose a parametric approximation method

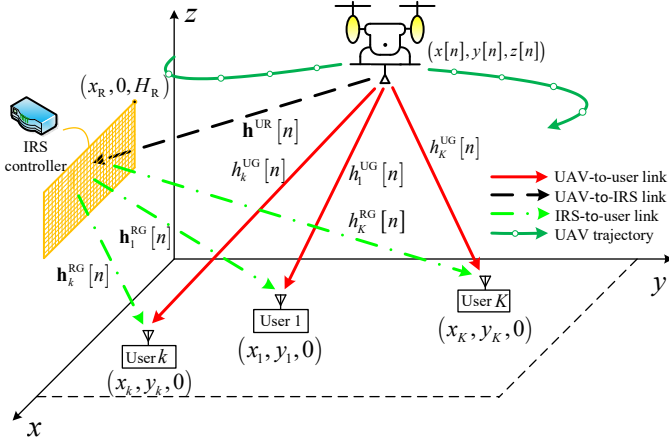


Fig. 1. The system model of the proposed IRS-assisted UAV communication systems.

to obtain a lower bound problem for the formulated problem. An alternating optimization approach is adopted to facilitate the development of a suboptimal iterative algorithm. Through simulations, we demonstrate that employing an IRS in UAV OFDMA communication systems can substantially improve the system sum-rate.

Notations: Boldface capital and lower case letters are reserved for matrices and vectors, respectively. $\mathbb{C}^{M \times N}$ denotes the set of all $M \times N$ matrices with complex entries; $(\cdot)^T$ denotes the transpose of a vector or a matrix and $(\cdot)^H$ denotes the Hermitian transpose of a vector or a matrix; $|\cdot|$ denotes the absolute value of a complex scalar or the cardinality of a set; and $\|\cdot\|$ denotes the Euclidean norm of a vector. $\mathbf{X} \otimes \mathbf{Y}$ represents the Kronecker product of two matrices \mathbf{X} and \mathbf{Y} ; $\text{diag}(\mathbf{x})$ denotes a diagonal matrix whose diagonal elements are given by its input vector \mathbf{x} . The circularly symmetric complex Gaussian distribution with mean μ and variance σ^2 is denoted by $\mathcal{CN}(\mu, \sigma^2)$.

II. SYSTEM MODEL

A. System Setup

We consider a single UAV serving as an aerial BS providing downlink communications to K ground users within a considered area, as shown in Fig. 1. Each ground user is equipped with a single-antenna. However, the single-antenna UAV is assisted by an IRS, which is located on the boundary of the considered service area. The IRS consists of $M_r \times M_c$ PRUs, which are spanned as a uniform planar array (UPA). In particular, each column of the UPA has M_c PRUs with an equal spacing of d_c meters and each row of the UPA consists of M_r PRUs with an equal spacing of d_r meters. Also, each PRU can re-scatter its incident signal with an independent reflection coefficient, $r_{m_r, m_c} = ae^{j\phi_{m_r, m_c}}$, $\forall m_r \in \{1, 2, \dots, M_r\}$ and $\forall m_c \in \{1, 2, \dots, M_c\}$. Note that variable $a \in [0, 1]$ models the fixed reflection loss of the IRS and $\phi_{m_r, m_c} \in [-\pi, \pi]$ denotes the phase shift inserted at PRU (m_r, m_c) , which can be adjusted by an external IRS controller¹.

¹In this work, we consider infinite resolution phase shifters at the IRS. Note that the extension to the case with low-resolution phase shifters will be considered in our future work by following a similar approach as in [11].

To facilitate the trajectory design, the total flying time of the UAV, T , is discretized into N time slots with an equal time interval, i.e., $\delta_t = \frac{T}{N}$. We assume that the distance between the UAV and each ground user is invariant within each time slot since it is much longer compared to the displacement of the UAV during δ_t [2]. Therefore, the three dimensional (3D) trajectory of UAV can be denoted as a sequence $\{\mathbf{q}[n] = [x[n], y[n], z[n]]^T\}_{n=1}^N$, where $\mathbf{q}[n]$ denotes the 3D coordinate of the UAV in time slot n . In practice, the UAV needs to satisfy the minimum flight altitude due to safety regulations, i.e., $z[n] \geq H_U$. The location of ground user k is assumed to be fixed and is denoted as $\mathbf{w}_k = [x_k, y_k, 0]^T$. The IRS is coated/installed on the surface of a building wall, which is usually located at the boundary of considered serving area with a certain altitude H_R , i.e., $\mathbf{w}_R = [x_R, 0, H_R]^T$. In time slot n , the distance between the UAV and ground user k is given by $d_k^{UG}[n] = \|\mathbf{q}[n] - \mathbf{w}_k\|$ and the distance between the UAV and the IRS is $d^{UR}[n] = \|\mathbf{q}[n] - \mathbf{w}_R\|$. Similarly, the distance between the IRS and ground user k is denoted as $d_k^{RG} = \|\mathbf{w}_R - \mathbf{w}_k\|$, which is assumed to be fixed in the considered system. Due to significant path loss and reflection loss, the power of the signals that are reflected by the IRS two or more times is negligible and thus is ignored in the system model [6].

B. Channel Model for IRS-assisted UAV OFDMA Systems

The total system bandwidth B is divided into N_F subcarriers with subcarrier spacing $\Delta f = \frac{B}{N_F}$. To facilitate the joint trajectory and resource allocation design, we assume line-of-sight (LoS)-dominated propagation² among the UAV, the IRS, and ground users [1], [2]. In time slot n , the channel vector between the UAV and the IRS on subcarrier i is given by [12]

$$\mathbf{h}_i^{UR}[n] = \sqrt{\beta_0}/d^{UR}[n] e^{-j2\pi i \Delta f \frac{d^{UR}[n]}{c}} \mathbf{h}_{\text{LoS}}^{UR}[n] \quad (1)$$

with $\mathbf{h}_{\text{LoS}}^{UR}[n]$ given by (2) on the top of next page, where β_0 denotes the channel power gain at the reference distance $d_0 = 1$ m, c denotes the speed of light, and f_c is the carrier frequency. And $\theta^{UR}[n]$ and $\xi^{UR}[n]$ denote the vertical and horizontal angles-of-arrival AoAs at the IRS, respectively³, with $\sin \theta^{UR}[n] = \frac{z[n] - H_R}{d^{UR}[n]}$, $\sin \xi^{UR}[n] = \frac{x_R - x[n]}{\sqrt{(x_R - x[n])^2 + (y_R - y[n])^2}}$, and $\cos \xi^{UR}[n] = \frac{y[n] - y_R}{\sqrt{(x_R - x[n])^2 + (y_R - y[n])^2}}$. We assume a far-field array response vector model at the IRS since $d^{UR}[n] \gg \max(M_r d_r, M_c d_c)$ holds in practice. Additionally, we note that the IRS interacts with a pass band signal with a carrier frequency f_c and a bandwidth B while $B \ll f_c$ holds usually, i.e., a narrow-band signal model in pass band. Therefore, the array response vector in (2) only depends on the corresponding AoAs and thus is frequency-flat [12]. In contrast, the phase shift term $e^{-j2\pi i \Delta f \frac{d^{UR}[n]}{c}}$ in (1) depends on the subcarrier

²Rician fading channel model will be considered in our journal version.

³Within a small time interval, we can assume that $\theta^{UR}[n]$ and $\xi^{UR}[n]$ do not change as $|x[n+1] - x[n]| \ll d^{UR}[n]$, $|y[n+1] - y[n]| \ll d^{UR}[n]$, and $|z[n+1] - z[n]| \ll d^{UR}[n]$ generally hold.

$$\mathbf{h}_{\text{LoS}}^{\text{UR}}[n] = \left[1, e^{-j2\pi f_c \frac{d_r \sin \theta^{\text{UR}}[n] \cos \xi^{\text{UR}}[n]}{c}}, \dots, e^{-j2\pi f_c (M_r-1) \frac{d_r \sin \theta^{\text{UR}}[n] \cos \xi^{\text{UR}}[n]}{c}} \right]^T$$

$$\otimes \left[1, e^{-j2\pi f_c \frac{d_c \sin \theta^{\text{UR}}[n] \sin \xi^{\text{UR}}[n]}{c}}, \dots, e^{-j2\pi f_c (M_c-1) \frac{d_c \sin \theta^{\text{UR}}[n] \sin \xi^{\text{UR}}[n]}{c}} \right]^T, \quad (2)$$

index⁴ even if all subcarriers' signal share the same delay $\frac{d^{\text{UR}}[n]}{c}$. In other words, a non-uniform phase is introduced to all subcarriers. This is fundamentally different from the existing literature considering only narrow-band IRS communications [6], [11], whereby the channel between transceiver can be characterized by a single complex number.

Similarly, in time slot n , the channel vector between the IRS and ground user k on subcarrier i is given by

$$\mathbf{h}_{k,i}^{\text{RG}}[n] = \sqrt{\beta_0} / d_k^{\text{RG}} e^{-j2\pi i \Delta f \frac{d_k^{\text{RG}}}{c}} \mathbf{h}_{k,\text{LoS}}^{\text{RG}} \quad (3)$$

with $\mathbf{h}_{k,\text{LoS}}^{\text{RG}}$ given by (4) on the top of next page, where θ_k^{RG} and ξ_k^{RG} denote angles-of-departure (AoDs) from the IRS to ground user k , respectively. Note that we have $\sin \theta_k^{\text{RG}} = \frac{H_{\text{R}}}{d_k^{\text{RG}}}$, $\sin \xi_k^{\text{RG}} = \frac{x_k - x_{\text{R}}}{\sqrt{(x_{\text{R}} - x_k)^2 + (y_{\text{R}} - y_k)^2}}$, and $\cos \xi_k^{\text{RG}} = \frac{y_k - y_{\text{R}}}{\sqrt{(x_{\text{R}} - x_k)^2 + (y_{\text{R}} - y_k)^2}}$. In time slot n , the channel between the UAV and ground user k on subcarrier i is given by

$$h_{k,i}^{\text{UG}}[n] = \sqrt{\beta_0} / d_k^{\text{UG}}[n] e^{-j2\pi i \Delta f \frac{d_k^{\text{UG}}[n]}{c}}. \quad (5)$$

In time slot n , the IRS reflection phase coefficient matrix can be represented by

$$\Phi[n] = \text{diag}(\phi[n]) \in \mathbb{C}^{M_r M_c \times M_r M_c}, \quad (6)$$

where $\phi[n] = [e^{j\phi_{1,1}[n]}, \dots, e^{j\phi_{m_r, m_c}[n]}, \dots, e^{j\phi_{M_r, M_c}[n]}]^T \in \mathbb{C}^{M_r M_c \times 1}$. In time slot n , the concatenation channel for the UAV-IRS-user link of user k on subcarrier i is given by

$$h_{k,i}^{\text{URG}}[n] = a (\mathbf{h}_{k,i}^{\text{RG}})^T \Phi[n] \mathbf{h}_i^{\text{UR}}[n]. \quad (7)$$

Now, the composite channel from the UAV to ground user k on subcarrier i in time slot n consists of two LoS paths in the UAV-to-user and the UAV-IRS-user links, respectively, and it can be given by

$$g_{k,i}^{\text{UG}}[n] = h_{k,i}^{\text{UG}}[n] + h_{k,i}^{\text{URG}}[n]. \quad (8)$$

C. Resource Allocation and IRS Scheduling

If user k is scheduled to subcarrier i in time slot n , we denote $u_{k,i}[n] = 1$. Otherwise, $u_{k,i}[n] = 0$. To guarantee the orthogonality among users on each subcarrier in each time slot, we impose $\sum_{k=1}^K u_{k,i}[n] \leq 1, \forall i, n$. Besides, the power allocated to user k on subcarrier i in time slot n is denoted as $p_{k,i}[n] \geq 0$ with $\sum_{i=1}^{N_{\text{F}}} \sum_{k=1}^K p_{k,i}[n] \leq p_{\text{max}}, \forall n$, where p_{max} denotes the maximum transmission power in each time slot. When user k is scheduled to be assisted by the IRS in time slot n , we define $s_k[n] = 1$. Otherwise, $s_k[n] = 0$. To achieve a considerable reflection gain at the IRS, we schedule at most one user to be assisted by the IRS in each time slot, i.e., $\sum_{k=1}^K s_k[n] \leq 1, \forall n$.

⁴The frequency domain channel for a discrete LoS channel $\delta[n - n_{\tau}]$ with a delay of $\tau = \frac{n_{\tau}}{N_{\text{F}}}$ can be obtained via performing an N_{F} -point discrete Fourier transform (DFT), i.e., $\text{DFT}\{\delta[n - n_{\tau}]\} = e^{-j2\pi \frac{i n_{\tau}}{N_{\text{F}}}} = e^{-j2\pi i \Delta f \tau}, \forall i \in \{0, \dots, N_{\text{F}} - 1\}$, where $\delta[\cdot]$ denotes the delta function.

III. PHASE CONTROL AND COMPOSITE CHANNEL GAIN

When allocating the IRS for user k in time slot n , i.e., $s_k[n] = 1$, the corresponding phase shift at PRU (m_r, m_c) is set as (9) on the top of next page. The adopted phase control strategy above is optimal for maximizing the passive beamforming gain at the IRS with respect to (w.r.t.) the IRS-assisted user. We can observe that the adopted simple phase control strategy in (9) only depends on the locations of UAV and ground users, which significantly reduces the required signaling overhead of CSI acquisition and phase control at the IRS [6]. Additionally, it can be seen that the phase control does not depend on the phase shift terms $e^{-j2\pi i \Delta f \frac{d_k^{\text{UG}}[n]}{c}}$ and $e^{-j2\pi i \Delta f \frac{d^{\text{UR}}[n] + d_k^{\text{RG}}}{c}}$ in each subcarrier. In fact, the phase control at IRS has a flat frequency response, which affects all the subcarriers homogeneously. Therefore, in general, we can only coherently combine the received signals from both the UAV-to-user link and the UAV-IRS-user link in some subcarriers as different subcarriers generally have different channel phases.

Substituting the phase control strategy (9) into (8), the composite channel power gain from the UAV to user k on subcarrier i in time slot n is given by equation (10) at the top of next page, where $\psi_{k',k}^{\text{r}} = \frac{\pi f_{\text{c}} d_{\text{r}} (\theta_{k'} - \theta_k)}{c}$, $\psi_{k',k}^{\text{c}} = \frac{\pi f_{\text{c}} d_{\text{c}} (\varphi_{k'} - \varphi_k)}{c}$, and the beam pattern function is $B_M(x) = \frac{\sin(Mx)}{\sin(x)}$. We can observe that the frequency-selective fading in (10) for both IRS-assisted and non-IRS-assisted users follows a periodic cosine pattern w.r.t. the subcarrier index. Furthermore, the period of the cosine fading pattern depends on the delay spread between the UAV-to-user link and the UAV-IRS-user link. One can imagine that the closer the IRS to the ground users, the longer the period of the frequency-selective fading. In particular, when the IRS is sufficiently close to the ground user, i.e., $d_k^{\text{RG}} \rightarrow 0$, we have $d^{\text{UR}}[n] \approx d_k^{\text{UG}}[n]$. In this case, the cosine function in (10) approaches a constant and $|g_{k,i}^{\text{UG}}[n]|^2$ becomes frequency-flat. In fact, when the employed IRS is sufficiently close to the ground users, it is expected that the UAV-to-user link and the UAV-IRS-user link almost merge with each other forming a pure LoS link with a frequency-flat characteristic. On the other hand, on each subcarrier, the composite channel gains for both the IRS-assisted and non-IRS-assisted users fluctuate with a cosine pattern w.r.t. the propagation distances' difference between the UAV-to-user link and the UAV-IRS-user link $d^{\text{UR}}[n] + d_k^{\text{RG}} - d_k^{\text{UG}}[n]$, as shown in (10), which is affected by the UAV's trajectory. As a result, the composite channel gain on one subcarrier also experiences a spatial-selective fading, which fluctuates along the UAV trajectory.

$$\mathbf{h}_{k,\text{LoS}}^{\text{RG}} = \left[1, e^{-j2\pi f_c \frac{d_r \sin \theta_k^{\text{RG}} \cos \xi_k^{\text{RG}}}{c}}, \dots, e^{-j2\pi f_c (M_r-1) \frac{d_r \sin \theta_k^{\text{RG}} \cos \xi_k^{\text{RG}}}{c}} \right]^T \otimes \left[1, e^{-j2\pi f_c \frac{d_c \sin \theta_k^{\text{RG}} \sin \xi_k^{\text{RG}}}{c}}, \dots, e^{-j2\pi f_c (M_c-1) \frac{d_c \sin \theta_k^{\text{RG}} \sin \xi_k^{\text{RG}}}{c}} \right]^T, \quad (4)$$

$$\phi_{m_r, m_c}[n] = 2\pi \frac{f_c}{c} \left\{ d_r (m_r - 1) \sin \theta_k^{\text{RG}} \cos \xi_k^{\text{RG}} + d_c (m_c - 1) \sin \theta_k^{\text{RG}} \sin \xi_k^{\text{RG}} + d_r (m_r - 1) \sin \theta^{\text{UR}}[n] \cos \xi^{\text{UR}}[n] + d_c (m_c - 1) \sin \theta^{\text{UR}}[n] \sin \xi^{\text{UR}}[n] \right\}. \quad (9)$$

$$\left| g_{k,i}^{\text{UG}}[n] \right|^2 = \left[\frac{\beta_0}{(d_k^{\text{UG}}[n])^2} + \sum_{k'=1}^K \frac{a^2 \beta_0^2 s_{k'}[n] B_{M_r}^2(\psi_{k',k}^{\text{r}}) B_{M_c}^2(\psi_{k',k}^{\text{c}})}{(d^{\text{UR}}[n])^2 (d_k^{\text{RG}})^2} + \sum_{k'=1}^K \frac{2a\beta_0^{\frac{3}{2}} s_{k'}[n] B_{M_r}(\psi_{k',k}^{\text{r}}) B_{M_c}(\psi_{k',k}^{\text{c}})}{d_k^{\text{UG}}[n] d^{\text{UR}}[n] d_k^{\text{RG}}} \right. \\ \left. \times \cos \left(2\pi i \Delta f \frac{d^{\text{UR}}[n] + d_k^{\text{RG}} - d_k^{\text{UG}}[n]}{c} + (M_r - 1) \psi_{k',k}^{\text{r}} + (M_c - 1) \psi_{k',k}^{\text{c}} \right) \right]. \quad (10)$$

IV. PROBLEM FORMULATION

A. Sum-rate Maximization Problem Formulation

In time slot n , the individual data rate of user k and the system sum-rate are given by

$$R_k[n] = \sum_{i=1}^{N_{\text{F}}} u_{k,i}[n] \log_2 \left(1 + p_{k,i}[n] \left| g_{k,i}^{\text{UG}}[n] \right|^2 / \sigma^2 \right) \text{ and} \\ R_{\text{sum}}[n] = \sum_{i=1}^{N_{\text{F}}} \sum_{k=1}^K u_{k,i}[n] \log_2 \left(1 + p_{k,i}[n] \left| g_{k,i}^{\text{UG}}[n] \right|^2 / \sigma^2 \right),$$

respectively, where $\sigma^2 = N_0 \Delta f$ denotes the noise power in each subcarrier and N_0 denotes the noise power spectral density at ground users. Now, the sum-rate maximization problem can be formulated as the following optimization problem:

$$\begin{aligned} \mathcal{P} : & \underset{\mathbf{U}, \mathbf{P}, \mathbf{q}[n], \mathbf{S}}{\text{maximize}} \frac{1}{N} \sum_{n=1}^N R_{\text{sum}}[n] (\mathbf{U}, \mathbf{P}, \mathbf{q}[n], \mathbf{S}) \\ \text{s.t. C1: } & u_{k,i}[n] \in \{0, 1\}, \forall k, i, n, \text{ C2: } \sum_{k=1}^K u_{k,i}[n] \leq 1, \forall i, n, \\ \text{C3: } & p_{k,i}[n] \geq 0, \forall k, i, n, \text{ C4: } \sum_{i=1}^{N_{\text{F}}} \sum_{k=1}^K p_{k,i}[n] \leq p_{\text{max}}, \forall n, \\ \text{C5: } & s_k[n] \in \{0, 1\}, \forall k, n, \text{ C6: } \sum_{k=1}^K s_k[n] \leq 1, \forall n, \\ \text{C7: } & \frac{1}{N} \sum_{n=1}^N R_k[n] (\mathbf{U}, \mathbf{P}, \mathbf{q}[n], \mathbf{S}) \geq R_{\text{min},k}, \forall k, \\ \text{C8: } & \|\mathbf{q}[n] - \mathbf{q}[n-1]\| \leq \delta_t V_{\text{max}}, \forall n, \\ \text{C9: } & \mathbf{q}[0] = \mathbf{q}_{\text{Initial}}, \quad \text{C10: } \mathbf{q}[N] = \mathbf{q}_{\text{Final}}. \end{aligned} \quad (11)$$

In the formulated problem in (11), constant $R_{\text{min},k}$ in C7 denotes the minimum required average data rate for user k during the whole flight period. Constraint C8 is imposed to make sure that the UAV's displacement in adjacent time slots is less than its maximum speed constraint V_{max} . Constraints C9 and C10 indicate the required UAV's initial location $\mathbf{q}_{\text{Initial}}$ and final location $\mathbf{q}_{\text{Final}}$, respectively.

Problem (11) is a non-convex mixed-integer optimization problem, which is generally difficult to solve. In particular, both the spatial and frequency-selective fading arising from the cosine function in the composite channel power gain in (10) makes (11) intractable, which has not been studied in the literature. In the following, as a compromise approach, we aim to find a lower bound problem of the formulated problem in (11) to facilitate our design.

B. Lower Bound Problem of (11)

In (11), we can observe that both the objective function and the left hand side of constraint C7 monotonically increase with the composite channel gain on each subcarrier. Inspired by this observation, we introduce an approximation parameter $0 < \alpha < \frac{1}{4}$ to quantize the cosine fading pattern of the composite channel gain in (10) into four-mode fading channels. In particular, when user k' is scheduled to be assisted by the IRS, i.e., $s_{k'}[n] = 1$, the composite channel gain of user k on subcarrier i in time slot n can be lower bounded by

$$\left| g_{k,k',i}^{\text{UG}}[n] \right|_{\text{LB}}^2 = \frac{\beta_0}{(d_k^{\text{UG}}[n])^2} + \frac{B_{k,k'}}{(d^{\text{UR}}[n])^2} + \frac{C_{k,k',i}}{d_k^{\text{UG}}[n] d^{\text{UR}}[n]}, \quad (12)$$

where $B_{k,k'} = a^2 \beta_0^2 B_{M_r}^2(\psi_{k',k}^{\text{r}}) B_{M_c}^2(\psi_{k',k}^{\text{c}}) / (d_k^{\text{RG}})^2$, $C_{k,k',i} = \sum_{j=1}^4 D_{k,k',j} I_{i,j}$, and $D_{k,k',j}$ is given by

$$D_{k,k',j} = \begin{cases} -\frac{2a\beta_0^{\frac{3}{2}} B_{M_r}(\psi_{k',k}^{\text{r}}) B_{M_c}(\psi_{k',k}^{\text{c}})}{d_k^{\text{RG}}} & \text{if } k' \neq k, \\ \frac{2a\beta_0^{\frac{3}{2}} M_r M_c}{d_k^{\text{RG}}} \cos(2\pi\alpha) & \text{if } k' = k, j = 1, \\ 0 & \text{if } k' = k, j = 2, \\ -\frac{2a\beta_0^{\frac{3}{2}} M_r M_c}{d_k^{\text{RG}}} \cos(2\pi\alpha) & \text{if } k' = k, j = 3, \\ -\frac{2a\beta_0^{\frac{3}{2}} M_r M_c}{d_k^{\text{RG}}} & \text{if } k' = k, j = 4. \end{cases} \quad (13)$$

Besides, binary variable $I_{i,j}$ is one if $i \in \mathcal{F}_j$ and is zero otherwise, where the subcarrier index sets for four fading mode are denoted as $\mathcal{F}_1 = \{1, \dots, 2\alpha N_{\text{F}}\}$, $\mathcal{F}_2 = \{2\alpha N_{\text{F}} + 1, \dots, \frac{1}{2}N_{\text{F}}\}$, $\mathcal{F}_3 = \{\frac{1}{2}N_{\text{F}} + 1, \dots, N_{\text{F}} - 2\alpha N_{\text{F}}\}$, and $\mathcal{F}_4 = \{N_{\text{F}} - 2\alpha N_{\text{F}} + 1, \dots, N_{\text{F}}\}$.

$\{N_F - 2\alpha N_F + 1, \dots, N_F\}$, respectively. Due to the page limitation, the detailed proofs about the lower bound in (12) are omitted here and left for our journal version.

Now, the following optimization problem provides a lower bound for the formulated problem in (11):

$$\mathcal{P}_{LB} : \underset{\mathbf{T}, \mathbf{U}, \mathbf{P}, \mathbf{q}[n], \mathbf{S}}{\text{maximize}} \frac{1}{N} \sum_{n=1}^N R_{\text{sum}}^{\text{LB}}[n] (\mathbf{T}, \mathbf{U}, \mathbf{P}, \mathbf{q}[n], \mathbf{S}) \quad (14)$$

s.t. C1-C6, C8-C10,

$$\underline{C7}: \frac{1}{N} \sum_{n=1}^N R_k^{\text{LB}}[n] (\mathbf{T}, \mathbf{U}, \mathbf{P}, \mathbf{q}[n], \mathbf{S}) \geq R_{\min, k}, \forall k,$$

$$\text{C11: } 0 \leq t_{k, k', i}[n] \leq 1, \forall k, k', n, i,$$

$$\text{C12: } t_{k, k', i}[n] \leq s_{k'}[n], \forall k, k', n, i,$$

$$\text{C13: } t_{k, k', i}[n] \leq u_{k, i}[n], \forall k, k', n, i,$$

$$\text{C14: } t_{k, k', i}[n] \geq s_{k'}[n] + u_{k, i}[n] - 1, \forall k, k', n, i,$$

where $t_{k, k', i}[n] = u_{k, i}[n] s_{k'}[n]$ is introduced to decouple the variables $u_{k, i}[n]$ and $s_{k'}[n]$. In particular, $t_{k, k', i}[n] = 1$ if and only if both $u_{k, i}[n] = 1$ and $s_{k'}[n] = 1$. Constraints C11-C14 are introduced to illustrate the relationship between $t_{k, k', i}[n]$, $u_{k, i}[n]$, and $s_{k'}[n]$. The system sum-rate can be obtained by $R_{\text{sum}}^{\text{LB}}[n] = \sum_{k=1}^K R_k^{\text{LB}}[n]$, where $R_k^{\text{LB}}[n] = \sum_{k'=1}^{N_F} \sum_{i=1}^N R_{k, k', i}^{\text{LB}}[n]$, and $R_{k, k', i}^{\text{LB}}[n]$ is given by

$$R_{k, k', i}^{\text{LB}}[n] = t_{k, k', i}[n] \log_2 \left(1 + p_{k, i}[n] |g_{k, k', i}[n]|_{\text{LB}}^2 / \sigma^2 \right). \quad (15)$$

V. SOLUTION OF THE LOWER BOUND PROBLEM

In this section, we aim to obtain a suboptimal solution of the lower bound problem \mathcal{P}_{LB} by dividing it into the following two subproblems, where we alternately solve the two subproblems until converge.

A. Subproblem 1: Resource Allocation and IRS Scheduling

Given the trajectory of the UAV $\mathbf{q}^{\text{iter}}[n]$ in the iter -th iteration, we have subproblem 1 as follows:

$$\underset{\mathbf{T}, \mathbf{U}, \mathbf{P}, \mathbf{S}}{\text{maximize}} \frac{1}{N} \sum_{n=1}^N R_{\text{sum}}^{\text{LB}}[n] (\mathbf{T}, \mathbf{U}, \mathbf{P}, \mathbf{S} | \mathbf{q}^{\text{iter}}[n]) \quad (16)$$

s.t. C1-C6, C7, C11-C14,

which is still a mixed-integer non-convex optimization problem. The binary variables $s_{k'}[n]$ and $u_{k, i}[n]$ span a disjoint feasible solution. To handle this, we relax the subcarrier allocation variable $u_{k, i}[n]$ and the IRS scheduling variable $s_{k'}[n]$ to be a real between zero and one instead of a Boolean. In fact, $u_{k, i}[n]$ and $s_{k'}[n]$ can be interpreted as time-sharing factors for subcarrier allocation and IRS scheduling, respectively [13]. As a result, $t_{k, k', i}[n] = u_{k, i}[n] s_{k'}[n]$ is a time-sharing factor for both subcarrier allocation and IRS scheduling. Besides, the coupling between optimization variables $t_{k, k', i}[n] = u_{k, i}[n] s_{k'}[n]$ and power allocation variables $p_{k, i}$ in the objective function and constraint in C7 is generally intractable. To tackle this, we introduce the

auxiliary time-shared power allocation variables $\tilde{p}_{k, k', i}[n] = t_{k, k', i}[n] p_{k, i}[n]$. The problem in (16) can be rewritten as

$$\underset{\mathbf{T}, \mathbf{U}, \tilde{\mathbf{P}}, \mathbf{S}}{\text{maximize}} \frac{1}{N} \sum_{n=1}^N R_{\text{sum}}^{\text{LB}}[n] (\mathbf{T}, \mathbf{U}, \tilde{\mathbf{P}}, \mathbf{S} | \mathbf{q}^{\text{iter}}[n]) \quad (17)$$

s.t. C2-C4, C6, C7, C11-C14,

$$\text{C1: } 0 \leq u_{k, i}[n] \leq 1, \forall k, i, n, \text{C5: } 0 \leq s_{k'}[n] \leq 1, \forall k', n,$$

$$\text{where } R_{\text{sum}}^{\text{LB}}[n] (\mathbf{T}, \mathbf{U}, \tilde{\mathbf{P}}, \mathbf{S} | \mathbf{q}^{\text{iter}}[n]) = R_{\text{sum}}^{\text{LB}}[n] (\mathbf{T}, \mathbf{U}, \mathbf{P}, \mathbf{S} | \mathbf{q}^{\text{iter}}[n]) \Big|_{p_{k, i}[n] = \frac{\tilde{p}_{k, k', i}[n]}{t_{k, k', i}[n]}},$$

The transformed problem in (17) is convex w.r.t. to $\mathbf{T}, \mathbf{U}, \tilde{\mathbf{P}}$, and \mathbf{S} , while satisfying the Slater's constraint qualification [14]. It can be solved efficiently by standard numerical solvers for convex programs, such as CVX [14]. Besides, it can be shown that the adopted binary constraint relaxation is tight [13] and thus the optimal solution of (16) is obtained.

B. Subproblem 2: UAV Trajectory Design

Given resource allocation and IRS scheduling design $(\mathbf{T}^{\text{iter}}, \mathbf{U}^{\text{iter}}, \tilde{\mathbf{P}}^{\text{iter}}, \mathbf{S}^{\text{iter}})$ in the iter -th iteration, defining $v_k^{\text{UG}}[n] = (d_k^{\text{UG}}[n])^2$ and $v^{\text{UR}}[n] = (d^{\text{UR}}[n])^2$ as slack variables for trajectory design results in the following optimization problem:

$$\underset{\mathbf{q}[n], \mathbf{v}_k^{\text{UG}}[n], \mathbf{v}^{\text{UR}}[n]}{\text{maximize}} \frac{1}{N} \sum_{n=1}^N \sum_{k=1}^K R_k^{\text{LB}}[n] (\mathbf{v}_k^{\text{UG}}[n], \mathbf{v}^{\text{UR}}[n] | \mathbf{T}^{\text{iter}}, \mathbf{U}^{\text{iter}}, \tilde{\mathbf{P}}^{\text{iter}}, \mathbf{S}^{\text{iter}}) \quad (18)$$

$$\text{s.t. } \underline{C7}, \text{C8-C10, C15: } v_k^{\text{UG}}[n] \geq \|\mathbf{q}[n] - \mathbf{w}_k\|^2, \forall n, k,$$

$$\text{C16: } v^{\text{UR}}[n] \geq \|\mathbf{q}[n] - \mathbf{w}_{\text{R}}\|^2, \forall n,$$

where constraints C15 and C16 hold with equality at the optimal solution since the closer the UAV to the ground users and the IRS, the higher the system sum-rate.

The transformed subproblem 2 in (18) is still non-convex and we employ an iterative algorithm based on successive convex approximation (SCA) technique [15], [16] to achieve a suboptimal solution. In particular, given a feasible solution $(\mathbf{v}_{k, l_{\text{II}}}^{\text{UG}}[n], \mathbf{v}_{l_{\text{II}}}^{\text{UR}}[n])$ in the l_{II} -th iteration, we have

$$\underset{\mathbf{q}[n], \mathbf{v}_k^{\text{UG}}[n], \mathbf{v}^{\text{UR}}[n]}{\text{maximize}} \frac{1}{N} \sum_{n=1}^N \sum_{k=1}^K R_k^{\text{LB}, l_{\text{II}}}[n] (\mathbf{v}_k^{\text{UG}}[n], \mathbf{v}^{\text{UR}}[n] | \mathbf{T}^{\text{iter}}, \mathbf{U}^{\text{iter}}, \tilde{\mathbf{P}}^{\text{iter}}, \mathbf{S}^{\text{iter}}) \quad (19)$$

$$\text{s.t. } \underline{C7}: \frac{1}{N} \sum_{n=1}^N R_k^{\text{LB}, l_{\text{II}}}[n] (\mathbf{v}_k^{\text{UG}}[n], \mathbf{v}^{\text{UR}}[n] | \mathbf{T}^{\text{iter}}, \mathbf{U}^{\text{iter}}, \tilde{\mathbf{P}}^{\text{iter}}, \mathbf{S}^{\text{iter}}) \geq R_{\min, k}, \forall k,$$

C8-C10, C15, C16,

where $R_k^{\text{LB}, l_{\text{II}}}[n]$ denotes a lower bound of $R_k^{\text{LB}}[n]$ given a feasible solution $(\mathbf{v}_{k, l_{\text{II}}}^{\text{UG}}[n], \mathbf{v}_{l_{\text{II}}}^{\text{UR}}[n])$ in the l_{II} -th iteration, i.e., $R_k^{\text{LB}, l_{\text{II}}}[n] \leq R_k^{\text{LB}}[n]$. $R_k^{\text{LB}, l_{\text{II}}}[n]$ is obtained by computing the first order Taylor expansion at point $(\mathbf{v}_{k, l_{\text{II}}}^{\text{UG}}[n], \mathbf{v}_{l_{\text{II}}}^{\text{UR}}[n])$ and it is given by (20) at the top of next page.

$$R_k^{\text{LB},l_{\text{II}}}[n] \left(\mathbf{v}_k^{\text{UG}}[n], \mathbf{v}^{\text{UR}}[n] \middle| \mathbf{T}^{\text{iter}}, \mathbf{U}^{\text{iter}}, \tilde{\mathbf{P}}^{\text{iter}}, \mathbf{S}^{\text{iter}} \right) = R_k^{\text{LB}}[n] \left(\mathbf{v}_{k,l_{\text{II}}}^{\text{UG}}[n], \mathbf{v}_{l_{\text{II}}}^{\text{UR}}[n] \middle| \mathbf{T}^{\text{iter}}, \mathbf{U}^{\text{iter}}, \tilde{\mathbf{P}}^{\text{iter}}, \mathbf{S}^{\text{iter}} \right) \quad (20)$$

$$+ \sum_{i=1}^{N_{\text{F}}} \sum_{k'=1}^K \frac{-\frac{\tilde{p}_{k,k',i}^{\text{iter}}[n]}{\ln 2} \left[\left(\frac{\beta_0}{(v_{k,l_{\text{II}}}^{\text{UG}}[n])^2} + \frac{C_{k,k',i}}{(v_{k,l_{\text{II}}}^{\text{UG}}[n])^{\frac{3}{2}} \sqrt{v_{l_{\text{II}}}^{\text{UR}}[n]}} \right) (v_k^{\text{UG}}[n] - v_{k,l_{\text{II}}}^{\text{UG}}[n]) + \left(\frac{B_{k,k'}}{(v_{l_{\text{II}}}^{\text{UR}}[n])^2} + \frac{C_{k,k',i}}{(v_{l_{\text{II}}}^{\text{UR}}[n])^{\frac{3}{2}} \sqrt{v_{k,l_{\text{II}}}^{\text{UG}}[n]}} \right) (v^{\text{UR}}[n] - v_{l_{\text{II}}}^{\text{UR}}[n]) \right]}{\sigma^2 + \frac{\tilde{p}_{k,k',i}^{\text{iter}}[n]}{t_{k,k',i}^{\text{iter}}[n]} \left(\frac{\beta_0}{v_{k,l_{\text{II}}}^{\text{UG}}[n]} + \frac{B_{k,k'}}{v_{l_{\text{II}}}^{\text{UR}}[n]} + \frac{C_{k,k',i}}{\sqrt{v_{k,l_{\text{II}}}^{\text{UG}}[n]} \sqrt{v_{l_{\text{II}}}^{\text{UR}}[n]}} \right)}.$$

Algorithm 1 Proposed Joint Trajectory, IRS Scheduling, and Resource Allocation Algorithm

1: **Initialization**

Initialize the convergence tolerance ϵ , the iteration index $\text{iter} = 1$, the maximum number of iterations iter_{max} , and the trajectory of UAV $\mathbf{q}^{\text{iter}}[n]$ according to Fig. 2.

2: **repeat**

3: Solve the problem in (17) via the dual decomposition method. Output the IRS scheduling and resource allocation strategy $(\mathbf{T}^{\text{iter}}, \mathbf{U}^{\text{iter}}, \tilde{\mathbf{P}}^{\text{iter}}, \mathbf{S}^{\text{iter}})$ and the corresponding average system sum-rate $R_{\text{sum}}^{\text{LB}}(2 \times \text{iter} - 1) = \frac{1}{N} \sum_{n=1}^N R_{\text{sum}}^{\text{LB}}[n] (\mathbf{T}^{\text{iter}}, \mathbf{U}^{\text{iter}}, \tilde{\mathbf{P}}^{\text{iter}}, \mathbf{S}^{\text{iter}} | \mathbf{q}^{\text{iter}}[n])$.

4: Solve the problem in (19) iteratively based on SCA with the initialized trajectory as $\mathbf{q}^{\text{iter}}[n]$. Output the UAV trajectory $\mathbf{q}^{\text{iter}+1}[n]$ and the corresponding average system sum-rate $R_{\text{sum}}^{\text{LB}}(2 \times \text{iter}) = \frac{1}{N} \sum_{n=1}^N R_{\text{sum}}^{\text{LB}}[n] (\mathbf{q}^{\text{iter}+1}[n] | \mathbf{T}^{\text{iter}}, \mathbf{U}^{\text{iter}}, \tilde{\mathbf{P}}^{\text{iter}}, \mathbf{S}^{\text{iter}})$.

5: $\text{iter} = \text{iter} + 1$

6: **until** $\text{iter} = \text{iter}_{\text{max}}$ or $\frac{|R_{\text{sum}}^{\text{LB}}(2 \times \text{iter}) - R_{\text{sum}}^{\text{LB}}(2 \times (\text{iter}-1))|}{R_{\text{sum}}^{\text{LB}}(2 \times (\text{iter}-1))} \leq \epsilon$

The problem in (19) is a convex optimization problem and solving (19) provides a lower bound for subproblem 2 in (18). To tighten the obtained lower bound, we iteratively update $(\mathbf{v}_k^{\text{UG}}[n], \mathbf{v}^{\text{UR}}[n])$ which generates a sequence of feasible solutions converging to a stationary point of the problem [15] in (18). In particular, given $(\mathbf{v}_{k,l_{\text{II}}}^{\text{UG}}[n], \mathbf{v}_{l_{\text{II}}}^{\text{UR}}[n])$ in the l_{II} -th iteration, solving the problem in (19) generates a feasible solution for the next iteration $(\mathbf{v}_{k,l_{\text{II}}+1}^{\text{UG}}[n], \mathbf{v}_{l_{\text{II}}+1}^{\text{UR}}[n])$.

Now, the overall algorithm for joint trajectory, IRS scheduling, and resource allocation design can be obtained via solving the subproblems 1 and 2 alternately. A description of the overall algorithm is summarized in **Algorithm 1**. Such an iterative procedure will terminate when the maximum iteration number is reached or the improvement of the system sum-rate is smaller than a predefined convergence tolerance.

VI. SIMULATION RESULTS

In this section, we evaluate the performance of the proposed scheme via simulations. The simulation setups are summarized in Table I. The system layout and the locations of ground users as well as the IRS are illustrated in Fig. 2. For comparison, we consider the UAV in baseline scheme 1 with a straight line trajectory and is assisted by the IRS, as shown in Fig. 2. Also, we compare our proposed scheme with the conventional UAV OFDMA communication system without the assistance of the IRS, which is referred as baseline scheme 2.

A. The Impact of IRS on UAV's Trajectory Design

Fig. 2 compares the obtained trajectories of UAV for the proposed scheme (PS) and baseline schemes to demonstrate the impact of IRS on UAV's trajectory design. For the proposed scheme, two simulation cases with $M_r = M_c = 200$ and

TABLE I
SIMULATION PARAMETERS [1].

Notation	Value	Notation	Value	Notation	Value
K	3	M_r	[200, 500]	$R_{\min,k}$	1 bit/s/Hz
δ_t	1 s	M_c	[200, 500]	c	3×10^8 m/s
H_U	100 m	p_{\max}	35 dBm	N_0	-169 dBm/Hz
H_R	30 m	Δf	100 kHz	$\mathbf{q}[1]$	$[0, 0]^T$ m
N	50	V_{\max}	20 m/s	$\mathbf{q}[N]$	$[500, 500]^T$ m
a	0.9	N_F	1000	β_0	-50 dBW
f_c	3 GHz	B	100 MHz		

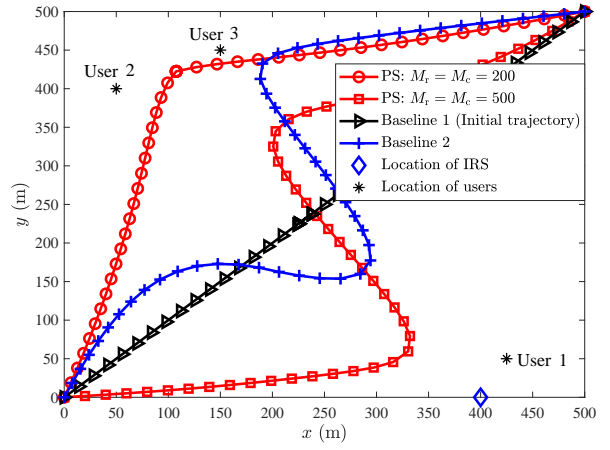


Fig. 2. Trajectory of UAV of difficult schemes.

$M_r = M_c = 500$, respectively, are conducted. For baseline 2, the UAV takes a time-consuming route who tries to approach each of all the three users in its route to establish strong communication links between them such that the ground users' minimum data rate requirements can be satisfied. In contrast, when equipping an IRS with $M_r = M_c = 200$, the UAV in the proposed scheme has a higher flexibility in designing its trajectory. Instead of flying to user 1, the UAV would directly fly towards a centroid formed by user 2 and user 3 for maximizing the system sum-rate. This is because the IRS located near user 1 can collect the dissipated radio power from the UAV and reflect it to user 1 through the proposed phase control for enhancing the composite power gain of user 1. In other words, the minimum data rate constraint of user 1 can still be satisfied even if the UAV is far away from it. When $M_r = M_c = 500$, the UAV in our proposed scheme would first approach closely to the IRS and user 1 at the beginning before flying close to users 2 and 3. In fact, equipping more PRUs allows the IRS to reflect the radiated signal more efficiently and thus the UAV approaching the IRS and user 1 becomes more beneficial to the system sum-rate performance. Therefore, compared to baseline 2, the UAV in

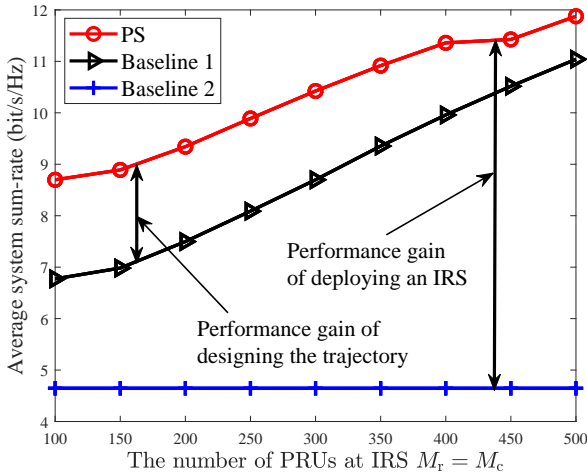


Fig. 3. Average system sum-rate (bit/s/Hz) versus the number of PRUs.

our proposed scheme flies towards user 1 and the IRS and stays close to them for a longer duration for achieving a higher system sum-rate.

B. Average System Sum-rate versus the Number of PRUs

Fig. 3 depicts the average system sum-rate versus the number of PRUs at the deployed IRS. We can observe that the system sum-rates of both the proposed scheme and baseline 1 increase with the increasing number of PRUs due to the enhanced passive beamforming gain achieved by our proposed phase control. Compared to baseline 1, a considerable sum-rate gain can be obtained by the proposed scheme due to the high flexibility of the UAV in trajectory design, as discussed in Fig. 2. Besides, a significant sum-rate gain of the proposed scheme over baseline 2 can be observed due to the energy focusing capability of the deployed IRS. Furthermore, it can be observed that the performance gain of the proposed scheme over baseline 1 slightly decreases with the increasing numbers of PRUs. This is because the IRS's passive beamforming gain is magnified by increasing M_r and M_c . As a result, the IRS can efficiently assist any user in need and the associated performance gain starts dominating the gain brought by UAV's trajectory optimization.

VII. CONCLUSIONS

In this paper, we proposed a novel IRS-assisted UAV OFDMA communication system and studied its joint trajectory, IRS scheduling, and resource allocation design to maximize the system sum-rate. With deploying an IRS on the boundary of the serving area, the composite channel power gain from the UAV to ground users becomes both frequency- and spatial-selective, which imposes a challenge for UAV's trajectory design. Via exploiting the cosine pattern in the frequency-selective composite channels, we proposed a parametric approximation method to generate a lower bound problem for the formulated problem. To obtain a suboptimal solution of the lower bound problem, an alternating optimization approach was adopted to design the resource allocation and IRS scheduling strategy as well as the UAV's trajectory. Extensive simulations were conducted to demonstrate the

system sum-rate improvement achieved by deploying an IRS in a UAV OFDMA communication system.

REFERENCES

- [1] Y. Zeng, Q. Wu, and R. Zhang, "Accessing from the sky: A tutorial on UAV communications for 5G and beyond," *Proceedings of the IEEE*, vol. 107, no. 12, pp. 2327–2375, Dec. 2019.
- [2] Y. Cai, Z. Wei, R. Li, D. W. K. Ng, and J. Yuan, "Joint trajectory and resource allocation design for energy-efficient secure UAV communication systems," *IEEE Trans. Commun.*, pp. 1–1, early access, Mar. 2020.
- [3] Q. Wu, Y. Zeng, and R. Zhang, "Joint trajectory and communication design for multi-UAV enabled wireless networks," *IEEE Trans. Wireless Commun.*, vol. 17, no. 3, pp. 2109–2121, Mar. 2018.
- [4] W. Yuan, C. Liu, F. Liu, S. Li, and D. W. K. Ng, "Learning-based predictive beamforming for UAV communications with jittering," early access, 2020.
- [5] M. Di Renzo, M. Debbah, D.-T. Phan-Huy, A. Zappone, M.-S. Alouini, C. Yuen, V. Sciancalepore, G. C. Alexandropoulos, J. Hoydis, H. Gacanin *et al.*, "Smart radio environments empowered by reconfigurable AI meta-surfaces: an idea whose time has come," *EURASIP J. Wireless Commun. and Networking*, vol. 2019, no. 1, pp. 1–20, 2019.
- [6] Q. Wu and R. Zhang, "Intelligent reflecting surface enhanced wireless network via joint active and passive beamforming," *IEEE Trans. Wireless Commun.*, vol. 18, no. 11, pp. 5394–5409, Nov. 2019.
- [7] B. Li, Z. Fei, and Y. Zhang, "UAV communications for 5G and beyond: Recent advances and future trends," *IEEE Internet Things J.*, vol. 6, no. 2, pp. 2241–2263, Apr. 2019.
- [8] Q. Zhang, W. Saad, and M. Bennis, "Reflections in the sky: Millimeter wave communication with UAV-carried intelligent reflectors," in *Proc. IEEE Global Commun. Conf.*, Dec. 2019, pp. 1–6.
- [9] S. Li, B. Duo, X. Yuan, Y. Liang, and M. Di Renzo, "Reconfigurable intelligent surface assisted UAV communication: Joint trajectory design and passive beamforming," *IEEE Wireless Commun. Lett.*, pp. 1–1, early access, Jan. 2020.
- [10] L. Ge, P. Dong, H. Zhang, J. Wang, and X. You, "Joint beamforming and trajectory optimization for intelligent reflecting surfaces-assisted UAV communications," *IEEE Access*, vol. 8, pp. 78 702–78 712, 2020.
- [11] C. Huang, A. Zappone, G. C. Alexandropoulos, M. Debbah, and C. Yuen, "Reconfigurable intelligent surfaces for energy efficiency in wireless communication," *IEEE Trans. Wireless Commun.*, vol. 18, no. 8, pp. 4157–4170, Aug. 2019.
- [12] A. Alkhateeb and R. W. Heath, "Frequency selective hybrid precoding for limited feedback millimeter wave systems," *IEEE Trans. Commun.*, vol. 64, no. 5, pp. 1801–1818, May 2016.
- [13] D. W. K. Ng, E. S. Lo, and R. Schober, "Wireless information and power transfer: Energy efficiency optimization in OFDMA systems," *IEEE Trans. Wireless Commun.*, vol. 12, no. 12, pp. 6352–6370, Dec. 2013.
- [14] S. Boyd and L. Vandenberghe, *Convex optimization*. Cambridge university press, 2004.
- [15] Z. Wei, L. Zhao, J. Guo, D. W. K. Ng, and J. Yuan, "Multi-beam NOMA for hybrid mmwave systems," *IEEE Trans. Commun.*, vol. 67, no. 2, pp. 1705–1719, Feb. 2019.
- [16] Z. Wei, D. W. K. Ng, J. Yuan, and H. M. Wang, "Optimal resource allocation for power-efficient MC-NOMA with imperfect channel state information," *IEEE Trans. Commun.*, vol. 65, no. 9, pp. 3944–3961, Sep. 2017.